Bandwidth-efficient visible light communication system based on faster-than-Nyquist pre-coded CAP modulation

Nan Chi (迟 楠)*, Jiaqi Zhao (赵嘉琦), and Zhixin Wang (王智鑫)

State Key Lab of ASIC, Department of Communication Science and Engineering, Fudan University, Shanghai 200433, China

**Corresponding author: nanchi@fudan.edu.cn*

Received February 20, 2017; accepted April 14, 2017; posted online May 15, 2017

With the rapid development of the light-emitting diode (LED) industry, interest in visible light communication (VLC) is growing. The limited bandwidth of commercial LEDs is one of the main challenges to achieve high-speed VLC. In this Letter, a kind of bandwidth-efficient VLC system based on carrierless amplitude and phase (CAP) modulation is proposed, where a simple differential faster-than-Nyquist (FTN) pre-coding scheme is employed to compress the spectrum and further improve the overall system baud rate. The system is experimentally demonstrated with a data rate of 1.47-Gb/s over 1.5 m free space transmission. The results indicate that an improvement of 80 Mbaud is achieved by FTN-CAP4 at 20% subband overlap and 40 Mbaud rate improvement by FTN-CAP16 at 7.5% subband overlap. Compared with traditional CAP, the FTN pre-coded CAP shows a better performance in spectral efficiency (SE) and intercarrier interference resistance. To the best of our knowledge, it is the first time to employ FTN pre-coded CAP in indoor high-data-rate VLC systems.

OCIS codes: 060.2605, 060.4510, 230.3670.
doi: 10.3788/COL201715.080601.

Light-emitting diode (LED)-based visible light communication (VLC) has been considered as a promising technology for future wireless communication, due to its unique advantages, such as low cost, low power consumption, free license, and high security[1]. A large number of investigations have been carried out for different VLC applications, especially indoor multi-user high-speed wireless access[2–6]. However, the limited bandwidth of commercial LEDs constrains the transmission data rate. To solve the problem, advanced modulation formats have been utilized, such as carrierless amplitude and phase (CAP)[6], discrete multi-tone (DMT)[7], and Nyquist single carrier (N-SC)[8]. Among them, CAP modulation is considered as a promising technique due to its low complexity and high spectral efficiency (SE). Recently, an 8 Gb/s VLC system employing high-order CAP modulation with hybrid post equalizers was experimentally demonstrated[9], which is the highest data rate ever achieved in CAP-based VLC systems. Moreover, Wang *et al.*[5,10] and have respectively demonstrated the feasibility of multiband CAP modulation in high-speed multi-user VLC access for its flexible allocation of user numbers and each user's bandwidth.

The performance of multiband CAP is influenced by out-of-band emission (OOBE), which brings about strong intercarrier interference (ICI). Therefore, like orthogonal frequency division multiplexing (OFDM), traditional multiband CAP needs to sacrifice some available modulation bandwidth as a guard band to suppress ICI. Recently, relaxing the orthogonality of the symbol period in the time domain has been found to be an effective way to reduce OOBE, and faster-than-Nyquist (FTN) is one of the useful methods reported in Refs. [11,12], where additional lowpass filters (LPFs) are added for regular Nyquist pulse generation[13]. As a result, the carrier spacing can be further reduced even less than the baud rate. In terms of multiband CAP, FTN is also a promising method. By employing an appropriate filtering and pre-coding process, the guard band consumption can be reduced to a minimum level and even appropriate overlap is available[14]. As a result, it is able to provide a higher level of SE and simultaneously support multi-user access and high data rate transmission.

In this Letter, to further improve the SE, we have proposed a novel FTN pre-coded CAP modulation scheme in the high-speed multi-user VLC system. A simple differential FTN pre-coding scheme is used to compress the spectrum and improve the overall system baud rate. Its feasibility is experimentally demonstrated by a 1.47 Gb/s visible light link over a 1.5 m free-space transmission. When considering the 7% forward error correction (FEC) threshold of 3.8×10^{-3}, the results indicate that an increase of 80 Mbaud is achieved by FTN-CAP4 at 20% subband overlap and an increase of 40 Mbaud is achieved by FTN-CAP16 at 7.5% subband overlap. The trade-off between SE performance and system baud rate is also discussed in both CAP4 and CAP16. To the best of our knowledge, this is the first time FTN pre-coded multiband CAP modulation is used in indoor high-speed VLC systems.

According to the Nyquist intersymbol interference (ISI) criterion, the maximum bandwidth efficiency of 2 Baud/Hz could be achieved by an ideal rectangular pulse-shaping filter. However, the 'tail' of the time-domain signal is too long and too large. The proposed FTN pre-coding scheme could highly reduce the 'tail' through

combining two waveforms separated by one symbol interval. The time-domain expression is

$$g(t)=\frac{\sin\left[\frac{\pi}{T_s}\left(t+\frac{T_S}{2}\right)\right]}{\frac{\pi}{T_s}\left(t+\frac{T_S}{2}\right)}+\frac{\sin\left[\frac{\pi}{T_s}\left(t-\frac{T_S}{2}\right)\right]}{\frac{\pi}{T_s}\left(t-\frac{T_S}{2}\right)}, \quad (1)$$

whose simplification is

$$g(t)=\frac{4}{\pi}\left[\frac{\cos\frac{\pi t}{T_s}}{1-\frac{4t^2}{T_s^2}}\right]. \quad (2)$$

The corresponding frequency characteristics obtained by Furier transform is

$$G(\omega)=\begin{cases}2T_s\cos\frac{\omega T_s}{2}, |\omega|\le\frac{\pi}{T_s},\\ 0, |\omega|\le\frac{\pi}{T_s}.\end{cases} \quad (3)$$

Thus, the spectrum is suppressed in $(-\frac{\pi}{T_s},\frac{\pi}{T_s})$, which achieves the Nyquist bandwidth. Furthermore, the spectrum shows slow half-cosine filter characteristics that could tolerate more subband overlap in multi-user systems and provides a higher SE.

Figure 1(a) shows the principle of the employed differential FTN pre-coding scheme. The original bit sequence is mapped into $2N$-quadrature amplitude modulation (QAM) first. Then the real part and imaginary part are respectively sent to differential coding, including modular operation, and delay. The signal after differential coding is expressed as

$$I_k=(i_k-I_{k-1})\mathrm{mod}N, \quad (4)$$

$$Q_k=(q_k-Q_{k-1})\mathrm{mod}N, \quad (5)$$

$$d_k=I_k+\mathrm{j}Q_k, \quad (6)$$

where i_k and q_k are the real and imaginary parts of the kth symbol of the generated $2N$-QAM signal. d_k is the kth symbol after differential coding. I_k and Q_k are the real and imaginary parts of d_k, respectively. $()\mathrm{mod}N$ means modular operation by the module value N. An additional delay and an add LPF follow behind the differential coding. The filter contains a two-tap finite impulse response (FIR) and can be simply implemented to turn quadrature phase shift keying (QPSK), 16QAM to 9QAM, and 49QAM, respectively[12], of which the transfer function in the z transform is given by

$$H(z)=1+z^{-1}. \quad (7)$$

In this way, the signal 3 dB bandwidth and OOBE is further suppressed to reduce the channel cross talk, as indicated in Fig. 1(b). The final FTN signal is expressed as

$$D_k=d_k+d_{k-1}. \quad (8)$$

For regular FTN filtering, only a two-tap FIR LPF is used in the signal generation indicated in Eq. (4). The proposed differential FTN pre-coding scheme adds an additional differential coding process, leading to a simpler receiver where only one modular operation is needed to realize differential decoding. Thus, the extra computation complexity brought by FTN pre-coding can be reduced.

To provide a clearer comparison, Table 1 lists the computation complexity of differential coding, FTN coding, decoding, and the regular CAP, respectively. Here, we take the 'I' branch for example. N is the length of the transmitted symbols, and n is the tap number of the FIR filters used in CAP transmitters and receivers, which is fixed at 33 in our system. So the total computation complexity of the regular CAP is $(2n-1)N=65N$ and that of FTN-CAP is $(2n+3)N=69N$. The additional computation brought by FTN-CAP is $4N$. Therefore, the complexity penalty of FTN-CAP is $4N/(65N)=6.2\%$. According to the results in our experiment, the maximum SE improvement achieved by FTN-CAP4 is 13%. Particularly, VLC is a bandwidth-limited system where the demand of higher SE is more urgent than that of the lower computation complexity. Hence, compared with the SE improvement of 13%, the additional computation complexity cost of 6.2% is relatively small and acceptable.

The ISI induced by optical multipath dispersion, sampling time offset, etc. seriously degrades the system performance. So a post equalizer is required to mitigate the interference. Series of post-equalization schemes, such as the cascaded multimodulus algorithm (CMMA)[6], modified CMMA (M-CMMA)[9], recursive least square (RLS)[15], and decision-directed least mean square (DD-LMS)[8], have been widely investigated and utilized in VLC systems. Among them, RLS is especially useful to

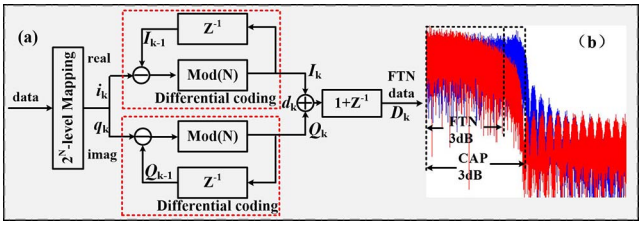

Fig. 1. (Color online) Principle diagram of the differential FTN pre-coding scheme.

Table 1. Computation Complexity of Each Step

Operation	Multiply	Plus	Sum
Differential coding	0	$2N$	$2N$
FTN coding	0	N	N
Decoding	0	N	N
Conventional CAP	$n\cdot N$	$(n-1)\cdot N$	$(2n-1)\cdot N$
FTN-CAP	$n\cdot N$	$(n+3)\cdot N$	$(2n+3)\cdot N$

VLC systems due to its quick convergence and modulation transparency[14]. In the system established in this Letter, only one RLS filter is adequate for the post equalization.

Figure 2 shows the experimental setup of the VLC system employing FTN pre-coding CAP and RLS post equalization. At the transmitting end, the original bit sequence is mapped into $2N$-QAM complex symbols first. Then the signal is sent into FTN pre-coding, including the differential coding module and delay and add filter module. After that, the coded QAM signal is sent into standard CAP modulation[16]. The roll-off coefficient of the square-root raised-cosine function for CAP modulation and demodulation is set at 0.02 to maximize the SE.

In this experiment, we use a Tektronix AWG 710 to generate the CAP signals, where the signal voltage peak-to-peak value (Vpp) is fixed at 0.4 V. The generated CAP signal is then pre-equalized by a self-designed bridged-T-based pre-equalizer to compensate the LED frequency attenuation[17], so that the LED modulation bandwidth is extended from several megahertz to about 350 MHz. Here, a commercial RGBY LED (LED Engine, output power: 1 W) is utilized as the transmitter. The LED driving voltage is fixed at 2.4 V[9]. After passing through an electrical amplifier (EA, minicircuits, 25 dB gain), the amplified electrical signal and direct current (DC) bias voltage are coupled by a bias tee (ZX85-12 G-S). The coupled signal is used to turn on the red chip of the LED and transmit information. A reflection cup with a 60° divergence angle is applied to decrease the beam angle of the LED for higher received optical power and longer transmission distance.

After 1.5 m free-space transmission, a commercial PIN photodiode (Hamamatsu 10784) is used as the receiver to complete the photoelectric conversion. In front of the PIN, a lens (50 mm diameter and 18 mm focus length) is used to focus a high proportion of light onto the PIN photosensitive surface. A transimpedance amplifier (TIA) receiving circuit is designed to amplify the weak electrical signal. Finally, the received signal is recorded by a digital storage oscilloscope (Agilent DSO54855A) for further offline digital signal processing (DSP).

In offline DSP, the electrical signal is sent into two digital match filters to separate the inphase and quadrature components. After downsampling, RLS algorithm is applied to mitigate the signal ISI. Then a simple modular operation is used to realize FTN decoding. In the end, the original bit sequence is recovered by QAM demapping.

First of all, we measure the bit error rate (BER) performance versus system baud rate of single-band CAP4 and single-band CAP16 with and without FTN and the results are shown in Fig. 3. When considering the BER threshold of 3.8×10^{-3}, a 470 Mbaud is achieved by regular CAP4 and a 490 Mbaud is achieved by FTN-CAP4. For CAP16, without FTN, the highest baud rate is 420 Mbaud, while with FTN, the baud rate is only 410 Mbaud. The results show that FTN-CAP4 provides about 20 Mbaud increase but FTN-CAP16 brings about 10 Mbaud decrease. It can be explained by the relationship between the occupied spectrum width and the minimum Euclidean distance of the constellation. When the signal spectrum is compressed by FTN, QPSK, and 16QAM are respectively turned into

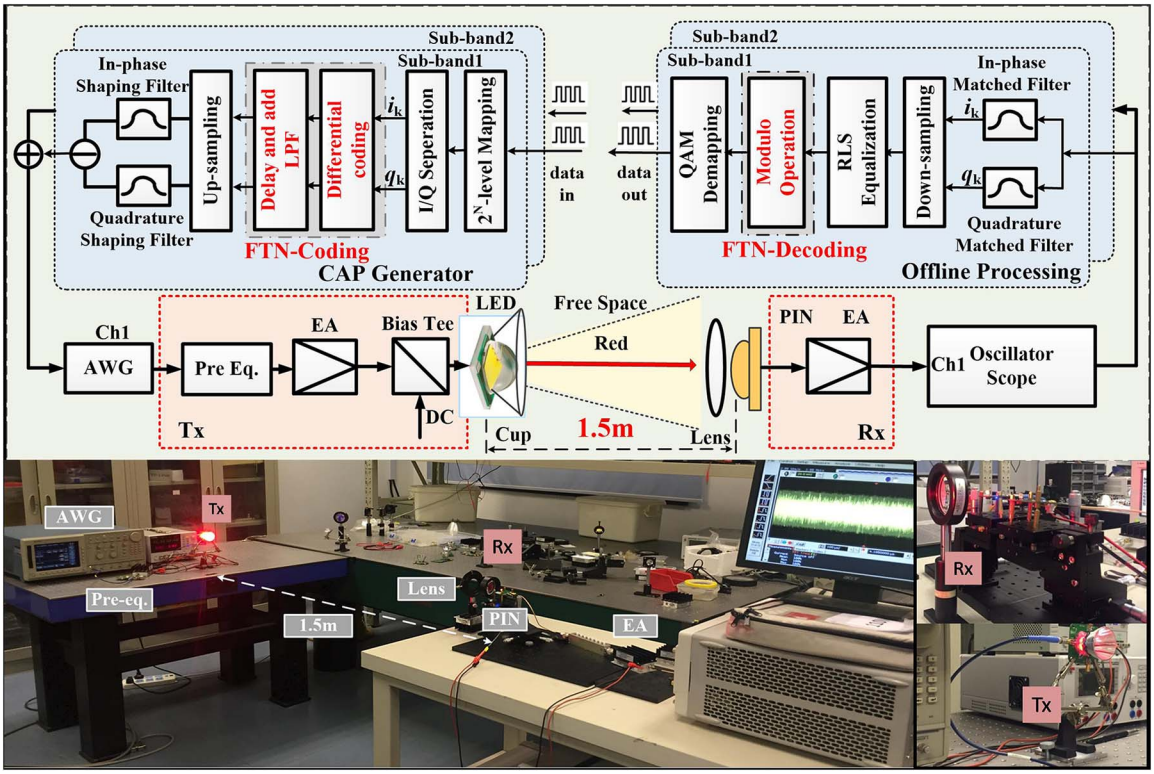

Fig. 2. Experimental setup of the VLC system.

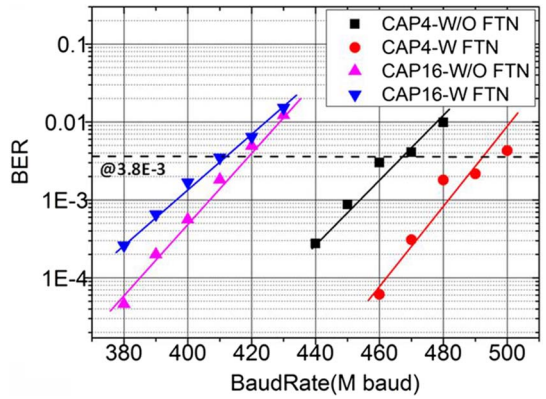

Fig. 3. (Color online) Measured BER versus system baud rate of the single-band CAP4 and CAP16W and with/without (W/O) FTN.

9QAM and 49QAM, as shown in Fig. 4. The compression of the spectrum is conducive to the system performance for its smaller bandwidth occupation. The increase of QAM order brings about the decrease of the Euclidean distance between adjacent constellation points, which will surely degrade the system performance. In terms of QPSK, the gain of spectrum suppression is greater than the loss of constellation deterioration. As a result, it has about a 20 Mbaud promotion. On the other hand, for 16QAM, the spectrum suppression gain is less than the Euclidean distance deterioration, because the signal-tonoise ratio (SNR) request of 49QAM is much higher than that of 16QAM. Thus, FTN-CAP16 not only provides no improvement but also results in about a 10 Mbaud reduction.

In the multiband CAP experiment, we investigate the influence of overlap between two subbands. Figure 4 shows the measured BER versus subband overlaps of two-band CAP4 and two-band CAP16 with and without FTN. The constellations of QPSK, 9QAM, 16QAM, 49QAM are presented in Fig. 4 as well. In Fig. 4(a), FTN-CAP4 can tolerate 37.5% subband overlap while regular CAP4 can only tolerate 23% subband overlap. In Fig. 4(b), system baud rate is fixed at 300 Mbaud. It shows that FTN-CAP16 can tolerate 15% subband overlap while regular CAP16 can tolerate 6% subband overlap. The performance improvement of subband 2 is smaller than that of subband 1 because of the high-frequency attenuation. The result indicates that, compared with regular CAP, FTN-CAP can achieve the same system baud rate with less modulation bandwidth cost, which means a higher SE. Furthermore, the FTN-CAP works more efficiently under the condition of sufficient SNR.

It can be explained by the signal spectrum of the two-band CAP16 without and with FTN at 10% subband overlap shown in Fig. 5. Figure 5(a) shows that, for regular CAP16, there is a peak between the joint of the two subbands. While Fig. 5(b) shows no peak in the spectrum, which indicates that FTN-CAP16 is slightly influenced

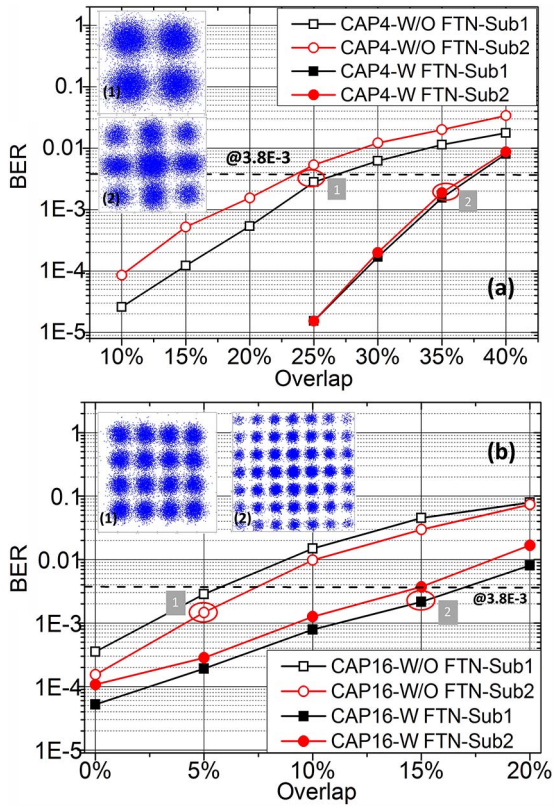

Fig. 4. (Color online) Measured BER versus subband overlaps of the (a) two-band CAP4 and (b) two-band CAP16W and W/O FTN.

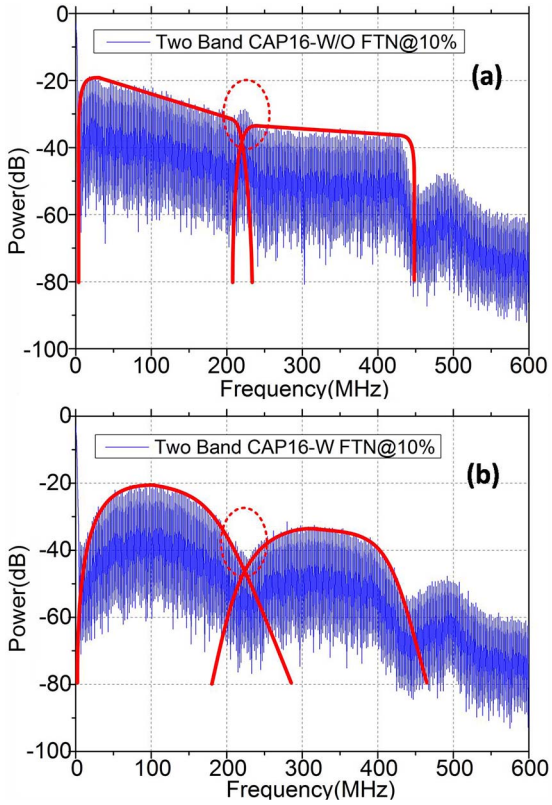

Fig. 5. (Color online) Measured signal spectrum of the two-band CAP16 (a) W/O and (b) W FTN at 10% subband overlap.

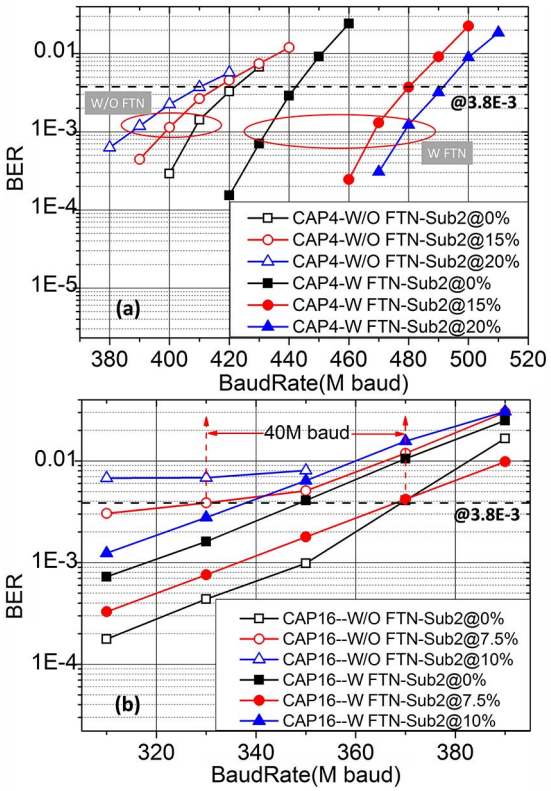

Fig. 6. (Color online) Measured BER versus system baud rate of the (a) two-band CAP4 and (b) two-band CAP16W and W/O FTN.

by the subband overlap because of the reduced OOBE. With the increase of overlap, the constellation points of the regular CAP signal are hardly separated due to the severe cross talk while FTN-CAP shows a great advantage in the tolerance of adjacent band overlap and provides a better resistance to ICI.

Figure 6 shows the measured BER performance versus the system baud rate of the two-band CAP4 and two-band CAP16 with and without FTN at different subband overlaps. With the increase of system baud rate, the performance of subband1 remains stable and the system BER is mainly decided by subband2. Therefore, only BER performance of subband2 is investigated in Fig. 6. Figure 6(a) indicates that FTN-CAP4 has about a 20 Mbaud promotion compared with CAP4 at 0% overlap. The result is the same with the single-band CAP4 shown in Fig. 3. When the overlap increases, the baud rate of the regular CAP decreases slightly, while the baud rate of FTN-CAP increases obviously, with an improvement of 80 Mbaud at 20% overlap.

Similarly, Fig. 6(b) shows that FTN-CAP16 has about 20 Mbaud deterioration compared with CAP16 at 0% overlap. When the overlap between two subbands increases, the baud rate of regular CAP16 decreases rapidly. At 10% overlap, the BER cannot satisfy the threshold of 3.8×10^{-3} even at a very low baud rate. However, the baud rate of FTN-CAP16 increases at 7.5% overlap and decreases at 10% overlap. 40 Mbaud promotion is obtained at 7.5% overlap. The results again prove that FTN-CAP performs higher SE quality compared with regular CAP.

According to the results shown in Fig. 6(b), it is found that there is a trade-off between SE and system baud rate. It could be explained by the limited bandwidth of the VLC system. On the one hand, when the overlap increases, the occupied bandwidth decreases so that the signal suffers less effects from the high-frequency attenuation and the BER gets better. On the other hand, when the overlap increases to a certain level, the ICI will become so severe that the BER gets worse. As the results shown in Fig. 7, the highest system baud rate of FTN-CAP4 is achieved at 27.5% overlap and the baud rate quickly declines after 30% overlap. At the same time, FTN-CAP16 reaches the highest baud rate at 7.5% overlap and quickly declines after 7.5% overlap. Eventually, the highest data rate is about 1.47 Gb/s, which is achieved by FTN-CAP16 with the baud rate of 367 Mbaud.

In this Letter, we propose a novel bandwidth-efficient VLC system based on FTN pre-coded CAP modulation. The feasibility and performance is experimentally demonstrated by a 1.47 Gb/s CAP modulated visible light link over 1.5 m free-space transmission. The experiment results indicate that FTN-CAP4 obtains an 80 Mbaud promotion at 20% subband overlap and FTN-CAP16 obtains a 40 Mbaud promotion at 7.5% subband overlap. Compared

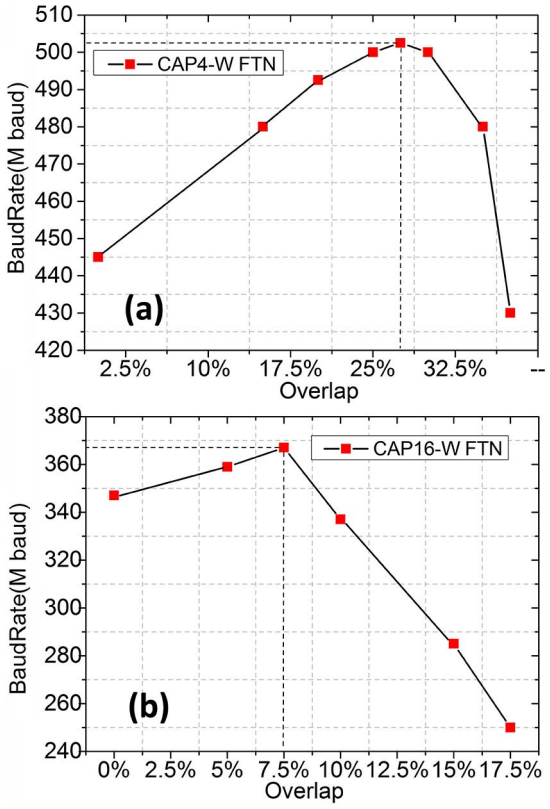

Fig. 7. Measured system baud rate versus overlap of the (a) two-band CAP4 and (b) two-band CAP16 with FTN.

with traditional CAP, FTN pre-coded CAP shows better SE performance and resistance to ICI. In addition, trade-off points between SE and system baud rate are experimentally obtained when the subband overlaps are 27.5% in CAP4 and 7.5% in CAP16. To the best of our knowledge, it is the first time FTN pre-coded multiband CAP modulation has been adopted in indoor high-speed VLC systems modulation. The advantage of multiband FTN-CAP verifies its potential in the application of existing indoor wireless access networks.

This work was supported by the National Science Foundation of China (No. 61571133) and the Key Project of Guangdong Province of China (No. 2015B010113001).

Reference

1. J. Luo, Y. Tang, H. Jia, Q. Zhu, and W. Xue, Chin. Opt. Lett. **14**, 120604 (2016).
2. J. Zhao, C. Qin, M. Zhang, and C. Nan, Photon. Res. **4**, 249 (2016).
3. C. Yang, Y. Wang, Y. Wang, X. Huang, and N. Chi, Opt. Commun. **336**, 269 (2015).
4. Z. Huang, C. Yan, K. Wu, and Y. Ji, Chin. Opt. Lett. **14**, 102301 (2016).
5. K. Cai and M. Jiang, in *2015 IEEE/CIC International Conference on Communications in China (ICCC)* (2015).
6. Y. Wang, L. Tao, Y. Wang, and N. Chi, IEEE Commun. Lett. **18**, 1719 (2014).
7. G. Cossu, A. Wajahat, R. Corsini, and E. Ciaramella, in *Proceedings of 40th European ECOC* (2014).
8. Y. Wang, X. Huang, J. Zhang, Y. Wang, and N. Chi, Opt. Express **22**, 15328 (2014).
9. Y. Wang, L. Tao, X. Huang, J. Shi, and N. Chi, IEEE Photon. J. **7**, 1 (2015).
10. P. A. Haigh, S. T. Le, S. Zvanovec, Z. Ghassemlooy, P. Luo, T. Xu, P. Chvojka, T. Kanesan, E. Giacoumidis, P. Canyelles-Pericas, H. L. Minh, W. O. Popoola, S. Rajbhandari, I. Papakonstantinou, and I. Darwazeh, IEEE Wireless Commun. **22**, 46 (2015).
11. C. Zhu, B. Corcoran, M. Morshed, L. Zhuang, and A. Lowery, in *Optical Fiber Communication Conference* (2015), paper Th3G-5.
12. W. Ding, F. Yang, S. Liu, and J. Song, IET Commun. **9**, 1606 (2015).
13. J. Yu, J. Zhang, Z. Dong, Z. Jia, H. C. Chien, Y. Cai, X. Xiao, and X. Li, Opt. Express **21**, 15686 (2013).
14. X. Huang, J.A. Zhang, and Y.J. Guo, IEEE Commun. Mag. **53**, 151 (2015).
15. Y. Wang, X. Huang, L. Tao, J. Shi, and N. Chi, Opt. Express **23**, 13626 (2015).
16. L. Tao, Y. Wang, Y. Gao, A. P. T. Lau, N. Chi, and C. Lu, Opt. Express **21**, 6459 (2013).
17. X. Huang, Z. Wang, J. Shi, Y. Wang, and N. Chi, Opt. Express **23**, 22034 (2015).